The classification, in 1997, by the International Agency for Research on Cancer (IARC) of certain forms of respirable crystalline silica (RCS) [1] as a category 1 carcinogen has led to the revision of a number of aspects relating to occupational protection against free silica. Thus, in 2003, the European Commission addressed the harmonisation of RCS exposure limits, proposing a value of 0.05 mg/m^3 as daily occupational exposure limit, which is 50% of the value currently in force in Spain. The reduction of the RCS occupational exposure limits makes it necessary to use increasingly sensitive analysis methodologies.

In this study, different analysis methodologies [2] were reviewed and a new methodology is proposed, using CIP 10-R personal samplers [3] and polyurethane foams, which allow the captured amount of powder to be increased with a flow rate up to 10 L/min, thus improving the detection and quantification limits.

The new methodology was validated in accordance with quality standard UNE-EN ISO/IEC 17025.

The proposed new methodology, using a CIP 10-R sampler, provides acceptable recovery and repeatability values. The methodology enables the detection limits attained by current methodologies (cyclone-type personal samplers with a 2 L/min flow rate) to be reduced to one fifth

The certified reference materials used to determine the traceability of the method were standard powders BCR-66 and SRM 1878a, and the standard powder deposited on filters SRM 2551-2557.

[1] The measurement of the exposure of workers to respirable crystalline silica (RCS) and the work of the international standard organisation (ISO). Working group TC146/SC2/WG7 Silica. P.R. Stacey IOHA **2005** [2] W.J, Miles, *American Industrial Hygiene Association Journal*, **1999**, *60 (3)*, 396-402. [3] T. Lee, S. Won Kim, W. P. Chisholm, J. Slaven, M. Harper. *Ann. Occup. Hyg*., **2010**, *54 (6),* 697–709.

Keywords: respirable crystalline silica (RCS), CIP 10-R, analytical methodology

MS32.P07

Acta Cryst. (2011) A**67,** C440

An study of the evolution of the NSA fertilizers with humidity

Jose Montejo-Bernardo, Santiago García-Granda, Alfonso Fernández-González, *Departament of Physical and Analytical Chemistry. University of Oviedo-CINN. Asturias (Spain).* E-mail: montejojose@uniovi.es

NSA fertilizers are formed mainly by the 2AN·AS and 3AN·AS double salts (AN: ammonium nitrate; AS: ammonium sulphate) [1], mixed in a determined range of percentages. But it is known that the 3AN·AS salt is meta-stable and evolves into the 2AN·AS salt [2]. Even though it is known that the evolution is catalyzed by the presence of humidity in the environment, this effect was not studied in deep.

In this work we analyze the evolution of the 3AN·AS salt in different humidity conditions in the presence of free AS salt. We analyze also the evolution of mixtures of AS and AN, in different proportions and in different humilities conditions. This work is an extension of a previous work, started sometime ago [3].

Results show the influence of the humidity conditions, the presence of free AS, the time of the experiment, and the initial amount of both double salts in the samples.

Analyses were made using XRPD data collected in an Agilent Nova diffractometer, with a CCD area detectors, and Rietveld fit. Acknowledgements: Spanish MICINN (MAT2006-01997, MAT2010-15094 and CSD2006-015, Consolider Ingenio 2010, “Factoría de Cristalización”) financial support and FEDER funding is acknowledged.

[1] J.M. Montejo-Bernardo, S. García-Granda, A. Fernández-González. *Acta Cryst. B*. **2010**. *66*, 358-365. [2] T. Y. Ling, C. K. Chan. *Environ. Sci. Technol*. **2007**, *41*, 8077-8083. [3] J.M. Montejo-Bernardo, S. García-Granda. *Book of abstract of the 2nd MISCA* **2010,** 126. Oviedo (Asturias, Spain).

Keywords: fertilizer, phase evolution, XRPD area detector

MS33.P01

Acta Cryst. (2011) A**67,** C440-C441

Crystalline structure identification by TEM with Microdiffraction, PED and CBED

Loïc Patout,[a] Jean-Sébastien Merot,[a] Giuseppe Pavia,[b] Gerd Benner,[b] Harald Niebel,[b] [a]*Laboratoire d'Etudes des Microstructures, Office Nationale des Etudes et Recherches en Aérospatiale, ONERA, Châtillon (France)*, [b]*Carl Zeiss NTS, Oberkochen (Germany).* E-mail: loic.patout@onera.fr

Microdiffration and Convergent Beam Electron Diffraction (CBED) are two techniques used in TEM to identify respectively the space and the point group of a crystal. One of the interests is to work with a small beam to overcome problems regularly met with the selected area diffraction such as the curvatures, faults and thicknesses variations.

Microdiffraction requires a slightly convergent beam with a nanometers probe size and this approach enables the Ewald sphere to probe several strata of the reciprocal lattice. Thus, when the sample is perfectly oriented in a zone axis, Microdiffraction patterns give access to ideal symmetries (position and intensity of diffracted beams), the gaps and the differences of periodicity between the Zero and the First Order Laue Zone. From this method, the space group of a crystalline sample is determined by identifying the Bravais lattice, the presence of glide mirrors and helicoidals axes depicted on some mains patterns [1].

Nevertheless, electron diffraction patterns are highly affected by dynamical effects due to the strong interaction of electrons with matter. Precession Electron Diffraction (PED) is a recent technique perfectly adapted to obtain more kinematical diffraction patterns by using a rocking beam illumination. Diffraction patterns obtained with a de-scanned precession of the incident beam contain as well more reflections and this allows to identify surely and easily the Bravais lattice and the glide mirrors [2].

CBED used with the Buxton or Tanaka (multibeam) methods allows to appreciate the symmetries inside the diffracted and incident disks of a slightly away from a perfect zone axis pattern. By comparing it with simulated patterns, the identification of the point group is then possible [3].

Both techniques were used to identify the space group $P6_3/mmc$ and the point group mmm of Ti_3SiC_2 and $TiSi_2$ respectively, two crystalline phases found by microanalysis (EELS, EDX and STEM HAADF). On one hand, CBED was very useful to find the point group mmm in working with only one zone axis. On the other hand, the space group Fddd has been determined in the same zone axis by Microdiffraction and PED.

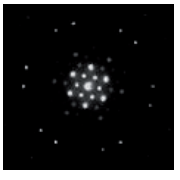

Fig.1: Microdiffraction

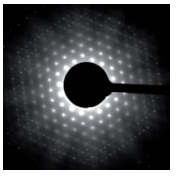

Fig.2: Precession

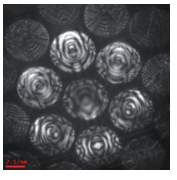

Fig.3: CBED Multibeam

[1] J.P. Morniroli, J.W. Steeds, *Ultramicroscopy* **1992**, *45*, 219-239. [2] R. Vincent, P.A. Midgley, *Ultramicroscopy* **1994,** *53*, 271-282. [3] M. Tanaka, M. Terauchi, *JEOL LTD*, **1985**, 156-159.

Keywords: microdiffraction, precession, multibeam

MS33.P02

Acta Cryst. (2011) A**67,** C441

The study of wide-angle incidence X-Ray nano-wires using crystal asymmetric surface diffraction

Hsin-Yi Chen,[a] Chia-Cheng Lin,[a] Yung-Shih Fang,[a] Yi-Wei Tsai,[a] Chia-Hung Chu,[a] and Shih-Lin Chang,[a,b] [a]*Department of Physics, National Tsing Hua University, Hsinchu, (Taiwan).* [b]*National Synchrotron Radiation Research Center, Hsinchu, (Taiwan).* E-mail: hychen@ms93.url.com.tw

Wide-angle incident x-ray Si-wires are devised by using crystal asymmetric surface diffraction. The Si (113) is chosen as an asymmetric surface diffraction for the photon energy 8.8785 keV according to the Si crystal orientation and diffraction geometry. The asymmetric surface diffracted beam propagates alone [110] if the incident beam is parallel to [110]. 2θ-scan (vertical) shows two diffraction peaks; one is the Si(113) Bragg diffraction, and the other is its surface specular reflection. The position of the specular reflection does not vary with photon energy in the range from E=9.05 keV to E=8.75 keV. The positions of these two peaks in vertical (2θ-scan) and horizontal (beta-scan) direction also depend on azimuth angle around [001], which is the angle between [110] and the incident-beam direction. The behavior of the diffracted beams in the vertical direction is governed by the photon energy and azimuth angle. In addition, interference patterns of specular reflection in the vertical direction are detected. The oscillatory intensity is related to the azimuth angle and extinction length, which we believe is a dynamical diffraction effect. The experimental results are in good agreement with the theoretical calculations using the dynamical theory of x-ray diffraction. In conclusion, we have studied the wide-angle incidence x-ray Si-wires using crystal asymmetric surface diffraction. This idea can be applied to design a new type wide-angle incidence x-ray optics using crystal surface diffraction.

Keywords: asymmetric-surface-diffraction

MS33.P03

Acta Cryst. (2011) A**67,** C441

Implementation of a direct approach to coherent diffractive imaging

Andrew J. Morgan,[a] Adrian J. D'Alfonso,[a] Andrew V. Martin,[b] Alexis I. Bishop,[c] Leslie J. Allen,[a] [a]*School of Physics, University of Melbourne, Victoria, (Australia).* [b]*Center for Free-Electron Laser Science, DESY, Hamburg (Germany).* [c]*School of Physics, Monash University, Victoria (Australia).* E-mail: andyofmelbourne@gmail.com

We present a strategy to obtain a high-fidelity reconstruction of the exit-surface wave of an object from its diffraction pattern. The direct solution of a set of linear equations extracted from the inverse Fourier transform of the diffraction pattern (which is the autocorrelation of the exit-surface wave) [1,2] is followed by a simple regularization step in which the solution is also made consistent with the non-linear information in the autocorrelation. This approach is illustrated using the diffraction pattern of a gnat's wing, illuminated with a laser. By considering residuals and condition numbers the well-posedness (uniqueness and consistency) of the reconstruction can be analyzed.

The figure below shows the results as follows: (a) The far-field diffraction pattern of a gnat's wing illuminated with a HeNe laser. (b) A magnified image of the gnat's wing. The black horizontal line indicates the area assumed to contain the object in the linear retrieval method. In (c) we have the retrieved intensity and in (d) the change in phase of the incident wave due to the wing after the solution of the linear equations and prior to the regularization step. After the regularization step we obtain the image shown in (e) and the phase in (f). In the figure the brightness of the phase images have been scaled by the wave's intensity.

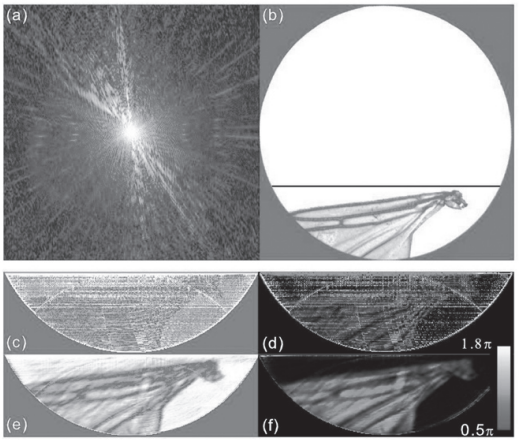

[1] A.V. Martin, L.J. Allen, *Optics Communications*, **2008**, *281*, 5114-5121 [2] A.V. Martin, A.I. Bishop, D.M. Paganin, L.J. Allen, *Ultramicroscopy*, **2011**, in press, doi:10.1016/j.ultramic.2010.10.003.

Keywords: coherence, diffraction, imaging

MS33.P04

Acta Cryst. (2011) A**67,** C441-C442

Observation of topography using resonant scattering and its SEM images

Riichirou Negishi,[a] Tomoe Fukamachi,[a] Kenji Hirano,[a] Yoshinobu Kanematsu,[a] Keiichi Hirano,[b] Takaaki Kawamura,[c] [a]*Saitama Institute of Technology,* [b]*KEK-PF,* [c]*University of Yamanashi (Japan).* E-mail; negishi@sit.ac.jp

Near the K-absorption edge of a constituent atom in a crystal, X-ray rocking curves from the crystal sometimes show significant change with small change of X-ray energy due to resonant scattering.

Fig.1 shows measured GaAs 200 diffracted rocking curves I_h, and transmitted ones I_t in Laue case[1] when X-ray energy is just below Ga K-edge (a) and 453.7eV below As K-edge (b). In (a), the rocking curves of I_h and I_t are anti-phase [2], while in (b), the maximum intensities due to anomalous transmission for I_h and I_t appear at the same angle and fringes in their tails are in-phase with each other. Figs. 2(a) and (b) shows
the topographs recorded at X-ray energies corresponding to those in Figs. 1(a) and (b), respectively. The interference fringes are clearly observed at the upper side of defect α (see arrow in (a)). The area around the defect α shows a dark band in (b).

Fig.3 shows a secondary electron image of the same region as in Fig.2 observed from the incident surface of X-ray by SEM (Scanning Electron Microscope). Along the defect band observed in the topographs in Fig. 2, many ditches are observed running in the [110] direction.

It is noted that topography making use of resonant scattering is very